# A time-staggered semi-Lagrangian discretisation of the rotating shallow-water equations*

ANDREW STANIFORTH†, NIGEL WOOD
*Met Office, Exeter, UK*
and
*SEBASTIAN REICH*
*Potsdam University, Germany*

5 July 2006

**Abstract**

A time-staggered semi-Lagrangian discretisation of the rotating shallow-water equations is proposed and analysed. Application of regularisation to the geopotential field used in the momentum equations leads to an unconditionally stable scheme. The analysis, together with a fully nonlinear example application, suggests that this approach is a promising, efficient, and accurate, alternative to traditional schemes.

KEYWORDS: Regularisation Temporal discretisation

## 1 Introduction

Recently, a novel time-staggered temporal discretisation of the rotating shallow-water equations (SWEs) has been proposed (Frank et al. 2005, Wood et al. 2006). Unconditional stability is achieved by appropriate regularisation of the geopotential field used in the momentum equations.

Whilst promising, the scheme and analysis of Frank et al. (2005) and Wood et al. (2006) neglected advection and any aspects of spatial discretisation. This paper therefore extends that work to include both effects: the temporal discretisation is coupled with a semi-Lagrangian (SL) scheme for advection and is discretised spatially on an Arakawa C-grid. The resulting scheme is second-order accurate in both time and space.

Linear analysis shows that unconditional stability is achieved provided a parameter governing the regularisation is chosen in the same way as for the non-advective scheme of Frank et al. (2005) and Wood et al. (2006). An example application of the scheme to a fully nonlinear case of two interacting vortices indicates the practical potential of the complete spatio-temporal discretisation.

After introducing the SWEs and describing the regularisation procedure in Sections 2 and 3, respectively, the application of a semi-Lagrangian scheme is detailed in Section 4. A linear analysis is presented in Section 5 and the example application, when the scheme is discretised spatially as detailed in the Appendix, is given in Section 6. Conclusions are given in Section 7.

## 2 The shallow-water equations

The shallow-water equations on an $f$-plane are

$$\frac{Du}{Dt} = +fv - \Phi_x, \tag{2.1}$$



† Corresponding author: Met Office, Fitzroy Road, Exeter, Devon EX1 3PB, UK

$$\frac{Dv}{Dt} = -fu - \Phi_y, \tag{2.2}$$

$$\frac{D\ln\Phi}{Dt} = -\mathfrak{D}, \tag{2.3}$$

where

$$\mathfrak{D} \equiv u_x + v_y, \tag{2.4}$$

is the horizontal divergence, $\Phi \equiv gh\,(x,y,t)$ is the height of the fluid above mean sea level multiplied by $g$ (the (constant) acceleration due to gravity), and $f$ is twice the (constant) angular velocity of the reference plane. Also, the kinematic equation is

$$\frac{D}{Dt}\,(x,y) = (u,v)\,, \tag{2.5}$$

where $u\,(x,y,t)$ and $v\,(x,y,t)$ are the wind components in the $x$ and $y$ directions respectively,

$$\frac{D}{Dt}\,(.) \equiv (.)_t + u\,(.)_x + v\,(.)_y\,, \tag{2.6}$$

is the material time derivative, and subscripts denote partial differentiation with respect to that variable. Eqs. (2.1) - (2.2) are the two components of the momentum equation and (2.3) is the continuity equation written in logarithmic form.

# 3 Regularisation

## 3.1 The regularisation procedure

For stability reasons, the governing equations (2.1) - (2.3) are regularised before discretisation by replacing $\Phi$ in the momentum equations by the regularised variable $\widetilde{\Phi}$ (Frank et al. 2005, Wood et al. 2006). Thus

$$\frac{Du}{Dt} = +fv - \widetilde{\Phi}_x, \tag{3.1}$$

$$\frac{Dv}{Dt} = -fu - \widetilde{\Phi}_y. \tag{3.2}$$

The Wood et al. (2006) regularisation, utilised herein, has the important advantage over the Frank et al. (2005) one of preserving dynamic balance, and only impacting the *unbalanced* components of the flow. It amounts, in continuous form [cf. (2.7)-(2.9) of Wood et al. (2006)], to solving the Helmholtz problem

$$\left(1-\alpha^2\nabla^2\right)\left(\widetilde{\Phi}-\Phi\right) = -\alpha^2\left(R_x^u + R_y^v\right), \tag{3.3}$$

where

$$R^u \equiv fv - \Phi_x,\ R^v \equiv -fu - \Phi_y, \tag{3.4}$$

$$\nabla^2 \equiv \partial_x^2 + \partial_y^2, \tag{3.5}$$

and $\alpha$ is a prescribed 'smoothing length scale'. Note that if the right-hand sides of (2.1) - (2.2) are identically zero, i.e. the winds are in geostrophic balance with the gradient of $\Phi$, then the regularisation (3.3) leaves $\Phi$ unchanged and the balanced state is preserved.

## 3.2 Linearisation of the regularised equations

To prepare for the analysis of the impact of regularisation on the propagation of linear inertia-gravity waves, (2.3) - (2.6) and (3.1) - (3.4) are linearised using the expansions

$$u\,(x,y,t) = U + u'\,(x,y,t)\,, \tag{3.6}$$

$$v\,(x,y,t) = V + v'\,(x,y,t)\,, \tag{3.7}$$

$$\Phi\,(x,y,t) = \Phi_0 + \Phi'\,(x,y,t)\,, \tag{3.8}$$

$$\widetilde{\Phi}\,(x,y,t) = \Phi_0 + \widetilde{\Phi}'\,(x,y,t)\,, \tag{3.9}$$

where primed variables are perturbations about the basic state, and $U$, $V$ and $\Phi_0$ are positive constants. [Implicit in this procedure is the inclusion of the gradients of an underlying bottom slope orography $h^S(x,y,t) = (fV/g)\,x - (fU/g)\,y$ in (3.1) - (3.2) in order to balance the mean velocity $(U,V)$ of the (stationary) basic-state. This permits analysis of the semi-Lagrangian aspects of the discretisation which would otherwise be omitted.] The linearisation then yields

$$\frac{D_L u'}{Dt} = +fv' - \widetilde{\Phi}'_x, \tag{3.10}$$

$$\frac{D_L v'}{Dt} = -fu' - \widetilde{\Phi}'_y, \tag{3.11}$$

$$\frac{D_L \Phi'}{Dt} = -\Phi_0 \mathfrak{D}', \tag{3.12}$$

where

$$\left(1 - \alpha^2 \nabla^2\right) \widetilde{\Phi}' = \Phi' - \alpha^2 f \zeta', \tag{3.13}$$

$$\zeta' \equiv v'_x - u'_y,\ \mathfrak{D}' \equiv u'_x + v'_y, \tag{3.14}$$

$$\frac{D_L}{Dt}(.) \equiv (.)_t + U(.)_x + V(.)_y. \tag{3.15}$$

### 3.3 Impact of regularisation on the propagation of linear inertia-gravity waves.

Inserting expansions of the form $\mathcal{F}(x,y,t) = \mathcal{F}_{k,l} \exp\left[i\left(kx + ly + \omega t\right)\right]$ into (3.10) - (3.15), where $\mathcal{F} = u', v', \Phi', \widetilde{\Phi}'$, it is straightforward to show that the impact of the regularisation procedure is to artificially reduce the frequency of linear inertia-gravity waves from $\omega = -(kU + lV) \pm \sqrt{f^2 + \Phi_0\left(k^2 + l^2\right)}$ to $\omega = -(kU + lV) \pm \sqrt{\left[f^2 + \Phi_0\left(k^2 + l^2\right)\right] / \left[1 + \alpha^2\left(k^2 + l^2\right)\right]}$. This analytic result, derived in Wood et al. (2006) for the special case $U \equiv V \equiv 0$, is independent of any discretisation procedure. It means that a spurious numerical dispersion is introduced into the continuous problem such that the highest wavenumber components are increasingly retarded as a function of increasing wavenumber (i.e., decreasing scale). This is similar to the impact of a semi-implicit discretisation of the original, unregularised equations, which also progressively retards the propagation of gravity modes as a function of decreasing scale (see e.g. Staniforth (1997)). Thus, the regularisation procedure qualitatively does at an analytic level what the semi-implicit method is known to do at a discrete level.

## 4 Time-staggered semi-Lagrangian discretisation

Eqs. (3.1), (3.2) and (2.3) are discretised using an explicit, time-staggered semi-Lagrangian discretisation of the governing equations, using values of $(u,v)$ defined at integer time levels "$n$", and values of $\Phi$ and $\widetilde{\Phi}$ defined at half-integer time levels "$n-1/2$". There are three steps to the discretisation which are repeatedly cycled. The first uses known gridpoint values of $(u,v)^{n-1}$ and $\widetilde{\Phi}^{n-1/2}$, to obtain gridpoint values of $(u,v)^n$. The second uses known gridpoint values of $\Phi^{n-1/2}$ and $(u,v)^n$ to obtain gridpoint values of $\Phi^{n+1/2}$. The third uses known gridpoint values of $(u,v)^n$ and $\Phi^{n+1/2}$ to obtain gridpoint values of $\widetilde{\Phi}^{n+1/2}$. These three steps are now described in detail.

### 4.1 Step 1, determination of $(u,v)^n$ from $(u,v)^{n-1}$ and $\widetilde{\Phi}^{n-1/2}$

Assume that $(x,y)_D^{n-1} \equiv \left(x\left(t^{n-1}\right), y\left(t^{n-1}\right)\right)$ denotes the location of a departure point for the velocity field at time $t^{n-1} \equiv (n-1)\,\Delta t$, where $\Delta t$ is the timestep length, $(x,y)_A^n$ denotes its corresponding gridpoint location at time $t^n \equiv n\Delta t$, and subscripts "$D$" and "$A$" signify evaluation at the departure and arrival points $\left(x\left(t^n\right), y\left(t^n\right)\right)$ and $\left(x\left(t^{n-1}\right), y\left(t^{n-1}\right)\right)$ respectively. The location of the departure point is determined using backward trajectories. Eq. (2.5) is thus discretised in a centred manner as

$$\frac{(x,y)_A^n - (x,y)_D^{n-1}}{\Delta t} = \frac{1}{2}\left[(u,v)_A^n + (u,v)_D^{n-1}\right], \tag{4.1}$$

where $(u,v)_D^{n-1}$ and $(u,v)_A^n$ correspond to the velocities at the departure and arrival points respectively.

The velocity $(u,v)_A^n$ is not however as yet known. Time-staggered semi-Lagrangian discretisations of (3.1) - (3.2) are therefore used to close the problem. Thus

$$\frac{u_A^n - u_D^{n-1}}{\Delta t} = +\frac{f}{2}\left(v_A^n + v_D^{n-1}\right) - \frac{1}{2}\left[\left(\widetilde{\Phi}_x\right)_A^{n-\frac{1}{2}} + \left(\widetilde{\Phi}_x\right)_D^{n-\frac{1}{2}}\right], \tag{4.2}$$

$$\frac{v_A^n - v_D^{n-1}}{\Delta t} = -\frac{f}{2}\left(u_A^n + u_D^{n-1}\right) - \frac{1}{2}\left[\left(\widetilde{\Phi}_y\right)_A^{n-\frac{1}{2}} + \left(\widetilde{\Phi}_y\right)_D^{n-\frac{1}{2}}\right], \tag{4.3}$$

where terms at time $(n-1/2)\,\Delta t$ are evaluated as the mean of their values at the arrival and departure points $\left(x\left(t^n\right), y\left(t^n\right)\right)$ and $\left(x\left(t^{n-1}\right), y\left(t^{n-1}\right)\right)$ respectively, and quantities at departure points are evaluated using interpolation.

The determination of values of $(u,v)^n$ from known values of $(u,v)^{n-1}$ and $\widetilde{\Phi}^{n-1/2}$ is a two-part procedure.

#### 4.1.1 Determination of trajectories for the discretisation of the momentum equations

To determine the position $(x,y)_D^{n-1}$ of departure points, discretisations (4.1) - (4.3) are solved iteratively using *bilinear* interpolation.

#### 4.1.2 Determination of $(u,v)_A^n$ from $(u,v)_D^{n-1}$ and $\widetilde{\Phi}^{n-1/2}$

Having determined $(x,y)_D^{n-1}$, the velocity $(u,v)_A^n$ at the arrival points is obtained from (4.2) - (4.3), where *bicubic* interpolation is now used instead of bilinear interpolation to evaluate quantities at the trajectory departure points $(x,y)_D^{n-1}$.

### 4.2 Step 2, determination of $\Phi^{n+1/2}$ from $\Phi^{n-1/2}$ and $(u,v)^n$

The determination of the backward trajectories for the discretisation of the continuity equation is done in the usual way (Staniforth & Côté 1991). Assume that $(x,y)_A^{n+1/2} \equiv \left(x\left(t^{n+1/2}\right), y\left(t^{n+1/2}\right)\right)$ denotes the location of an arrival point for $\Phi$ at time $(n+1/2)\,\Delta t$, $(x,y)_D^{n-1/2}$ denotes its corresponding departure location at time $(n-1/2)\,\Delta t$, and subscript "$D$" now denotes evaluation at the departure point of the trajectory used to discretise the *continuity* equation, instead of the *momentum* equation. The arrival point is assumed to be a gridpoint. The corresponding location $(x,y)_D^{n-1/2}$ of the departure point is determined using backward trajectories, i.e. by discretising (2.5) as

$$\frac{(x,y)_A^{n+\frac{1}{2}} - (x,y)_D^{n-\frac{1}{2}}}{\Delta t} = \frac{1}{2}\left[(u,v)_A^n + (u,v)_D^n\right]. \tag{4.4}$$

The determination of values of $\Phi^{n+1/2}$ from known values of $\Phi^{n-1/2}$ and $(u,v)^n$ is also a two-part procedure.

#### 4.2.1 Determination of trajectories for the discretisation of the continuity equation

To determine the position $(x,y)_D^{n-1/2}$ of departure points, discretisation (4.4) is solved iteratively using *bilinear* interpolation .

#### 4.2.2 Determination of $\Phi^{n+1/2}$ from $\Phi^{n-1/2}$ and $(u,v)^n$

Having determined $(x,y)_D^{n-1/2}$, $\Phi^{n+1/2}$ is determined from $\Phi^{n-1/2}$ and $(u,v)^n$ by using the following time-staggered discretisation of the continuity equation (2.3):

$$\frac{\ln\left(\Phi_A^{n+\frac{1}{2}}\right) - (\ln\Phi)_D^{n-\frac{1}{2}}}{\Delta t} = -\frac{1}{2}\left(\mathfrak{D}_A^n + \mathfrak{D}_D^n\right), \tag{4.5}$$

i.e.

$$\Phi_A^{n+\frac{1}{2}} = \exp\left\{\left[(\ln\Phi)^{n-\frac{1}{2}} - \frac{\Delta t}{2}\mathfrak{D}^n\right]_D - \frac{\Delta t}{2}\mathfrak{D}_A^n\right\}. \tag{4.6}$$

Here

$$\mathfrak{D}^n \equiv (u_x + v_y)^n, \tag{4.7}$$

and subscript " $D$" denotes evaluation using *cubic* interpolation at the trajectory departure point $(x,y)_D^{n-1/2}$.

### 4.3 Step 3, determination of $\widetilde{\Phi}_A^{n+1/2}$ from $\Phi_A^{n+1/2}$

The crucial step for stable propagation of gravitational oscillations with long time steps is the application of regularisation - see Frank et al. (2005) and Wood et al. (2006) for analysis of this and its link to the semi-implicit time scheme. This is accomplished by solving a Helmholtz problem to obtain $\widetilde{\Phi}_A^{n+1/2}$ for use in the regularised momentum equations (3.1) - (3.2) at the next timestep. Thus $\widetilde{\Phi}_A^{n+1/2}$ is obtained by solving the discrete Helmholtz problem (cf. (2.14) - (2.16) of Wood et al. (2006))

$$\left[1 - \left(\frac{\alpha^2}{1+F^2}\right)\nabla^2\right]\left(\widetilde{\Phi} - \Phi\right)_A^{n+1/2} = -\alpha^2\left(\mathcal{R}_x^u + \mathcal{R}_y^v\right), \tag{4.8}$$

where

$$\mathcal{R}^u \equiv \frac{f}{2}\left(v_A^n + v_D^n + \Delta t\mathcal{R}^v\right) - \left(\Phi_x\right)_A^{n+\frac{1}{2}}, \quad \mathcal{R}^v \equiv -\frac{f}{2}\left(u_A^n + u_D^n + \Delta t\mathcal{R}^u\right) - \left(\Phi_y\right)_A^{n+\frac{1}{2}}. \tag{4.9}$$

Eliminating $\mathcal{R}^u$ and $\mathcal{R}^v$ from (4.8) - (4.9) then leads to

$$\left[1 - \left(\frac{\alpha^2}{1+F^2}\right)\nabla^2\right]\widetilde{\Phi}_A^{n+1/2} = \Phi_A^{n+1/2} - \left(\frac{\alpha^2}{1+F^2}\right)\frac{f}{2}\left\{\left[\left(v_A^n + v_D^n\right)_x - \left(u_A^n + u_D^n\right)_y\right] - F\left[\left(u_A^n + u_D^n\right)_x + \left(v_A^n + v_D^n\right)_y\right]\right\}, \tag{4.10}$$

where $F \equiv f\Delta t/2$. The choice of an appropriate value for $\alpha$ is discussed in Section 5.2.

## 5 Analysis

### 5.1 Linearisation

The time-staggered semi-Lagrangian discretisation described in Section 4 is, in summary, comprised of (4.1) - (4.7) and (4.10). As the first step in the analysis, these equations are linearised using the expansions (3.6) - (3.9) to give

$$\frac{u_A'^n - u_D'^{n-1}}{\Delta t} = \frac{f}{2}\left(v_A'^n + v_D'^{n-1}\right) - \frac{1}{2}\left[\left(\widetilde{\Phi}_x'^{n-\frac{1}{2}}\right)_A + \left(\widetilde{\Phi}_x'^{n-\frac{1}{2}}\right)_D\right], \tag{5.1}$$

$$\frac{v_A'^n - v_D'^{n-1}}{\Delta t} = -\frac{f}{2}\left(u_A'^n + u_D'^{n-1}\right) - \frac{1}{2}\left[\left(\widetilde{\Phi}_y'^{n-\frac{1}{2}}\right)_A + \left(\widetilde{\Phi}_y'^{n-\frac{1}{2}}\right)_D\right], \tag{5.2}$$

$$\frac{\Phi_A'^{n+\frac{1}{2}} - \Phi_D'^{n-\frac{1}{2}}}{\Delta t} = -\frac{\Phi_0}{2}\left(\mathfrak{D}_A'^n + \mathfrak{D}_D'^n\right), \tag{5.3}$$

where

$$\left[1 - \left(\frac{\alpha^2}{1+F^2}\right)\nabla^2\right]\widetilde{\Phi}_A'^{n-1/2} = \Phi_A'^{n-1/2} - \left(\frac{\alpha^2}{1+F^2}\right)\frac{f}{2}\left[\left(\zeta_A'^{n-1} + \zeta_D'^{n-1}\right) - F\left(\mathfrak{D}_A'^{n-1} + \mathfrak{D}_D'^{n-1}\right)\right], \tag{5.4}$$

$$\zeta'^{n-1} \equiv v_x'^n - u_y'^n, \; \mathfrak{D}'^{n-1} \equiv u_x'^n + v_y'^n, \tag{5.5}$$

$$(x,y)_D^{n-1} = (x,y)_A^n - \Delta t\,(U,V), \tag{5.6}$$

$$(x,y)_D^{n-\frac{1}{2}} = (x,y)_A^{n+\frac{1}{2}} - \Delta t\,(U,V). \tag{5.7}$$

For analysis purposes, it is convenient to take the curl and divergence of (5.1) - (5.2) to obtain,

$$\frac{\zeta_A'^n - \zeta_D'^{n-1}}{\Delta t} = -\frac{f}{2}\left(\mathfrak{D}_A'^n + \mathfrak{D}_D'^{n-1}\right), \tag{5.8}$$

$$\frac{\mathfrak{D}_A'^n - \mathfrak{D}_D'^{n-1}}{\Delta t} = \frac{f}{2}\left(\zeta_A'^n + \zeta_D'^{n-1}\right) - \frac{1}{2}\left(\nabla^2\widetilde{\Phi}_A'^{n-\frac{1}{2}} + \nabla^2\widetilde{\Phi}_D'^{n-\frac{1}{2}}\right). \tag{5.9}$$

## 5.2 Stability

Stability of the discretisation is governed by (5.3) - (5.9). Note that (5.8) implies $\zeta_A'^n + F\mathfrak{D}_A'^n = \zeta_D'^{n-1} - F\mathfrak{D}_D'^{n-1}$, so that

$$\zeta_D'^{n-1} - F\mathfrak{D}_D'^{n-1} = \frac{1}{2}\left(\zeta_A'^n + \zeta_D'^{n-1}\right) + \frac{F}{2}\left(\mathfrak{D}_A'^n - \mathfrak{D}_D'^{n-1}\right). \tag{5.10}$$

This equation is used to simplify the linearised regularisation equation (5.4). Assume exact differentiation and interpolation and the time-dependent expansions

$$\mathcal{F}(x,y,t) = \mathcal{F}_{k,l}\exp\left[i\left(kx + ly + \omega t\right)\right], \tag{5.11}$$

where $\mathcal{F} = u', v', \zeta', \mathfrak{D}', \Phi', \tilde{\Phi}'$. Insertion of (5.11) into (5.3) - (5.9) and use of (5.10) then leads to

$$\mathcal{N}\begin{bmatrix} \zeta_{k,l}' \\ \mathfrak{D}_{k,l}' \\ \Phi_{k,l}' \end{bmatrix} \equiv \begin{bmatrix} (E-1) & F(E+1) & 0 \\ -RSF(E+1) & (E-1) & -\Delta t R\cos(\xi)\left(k^2+l^2\right)E^{\frac{1}{2}} \\ 0 & \cos(\xi)\,\Phi_0\Delta t E^{\frac{1}{2}} & (E-1) \end{bmatrix}\begin{bmatrix} \zeta_{k,l}' \\ \mathfrak{D}_{k,l}' \\ \Phi_{k,l}' \end{bmatrix} = 0, \tag{5.12}$$

where

$$E \equiv \exp\left[i\left(\omega + kU + lV\right)\Delta t\right],\ E_0 \equiv E(\omega = 0),\ \cos(\xi) \equiv \frac{E_0^{\frac{1}{2}} + E_0^{-\frac{1}{2}}}{2} = \cos\left[\left(kU + lV\right)\frac{\Delta t}{2}\right], \tag{5.13}$$

and

$$R \equiv \frac{1}{1 + \left[1 + F^2\cos^2(\xi)\right]\Lambda^2},\ S \equiv 1 + \sin^2(\xi)\,\Lambda^2,\ \Lambda^2 \equiv \frac{\alpha^2\left(k^2+l^2\right)}{1+F^2}. \tag{5.14}$$

Eqs. (5.6) - (5.7) have also been used to allow simplification of exponential terms.

For (5.12) to have non trivial solutions, the determinant of the matrix $\mathcal{N}$ must be zero which yields the dispersion relation

$$(E-1)\left[(E-1)^2 + RSF^2(E+1)^2 + 4RG^2\cos^2(\xi)\,E\right] = 0, \tag{5.15}$$

where

$$G^2 \equiv \Phi_0\left(\frac{\Delta t}{2}\right)^2\left(k^2+l^2\right). \tag{5.16}$$

The trivial root

$$E \equiv \exp\left[i\left(\omega + kU + lV\right)\Delta t\right] = 1, \tag{5.17}$$

corresponds to the degenerate Rossby mode, which is neutrally stable.

The other two roots correspond to gravity modes and they satisfy

$$(E-1)^2 + RSF^2(E+1)^2 + 4RG^2\cos^2(\xi)\,E = 0, \tag{5.18}$$

which, using (5.14), may be rewritten as

$$AE^2 - 2BE + C = 0, \tag{5.19}$$

where

$$A = C = R^{-1} + SF^2,\ B = R^{-1} - SF^2 - 2G^2\cos^2(\xi). \tag{5.20}$$

The solution of (5.19) is

$$E = \frac{B \pm i\sqrt{A^2 - B^2}}{A}, \tag{5.21}$$

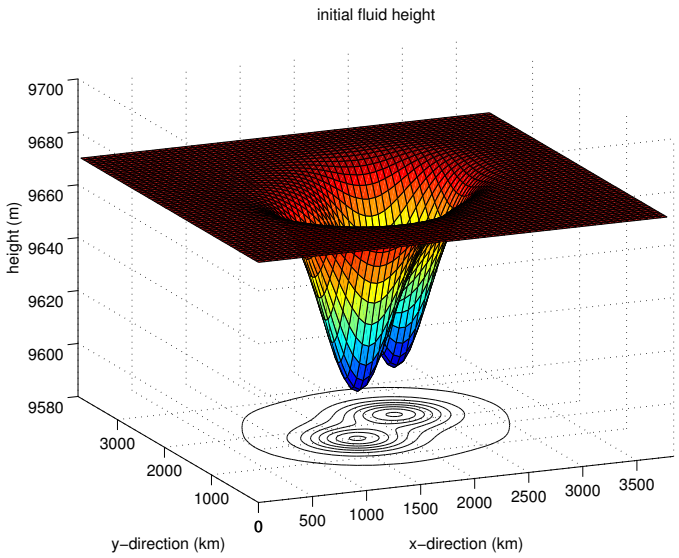


Figure 1: Initial fluid height $h$.

where

$$A^2 - B^2 = 4\left[SF^2 + G^2\cos^2(\xi)\right]\left[\frac{1}{R} - G^2\cos^2(\xi)\right]. \tag{5.22}$$

Since $A$ and $B$ are real, neutral stability (i.e. $|E| = 1$) is obtained provided the discriminant $A^2 - B^2 \geq 0$. Using the definitions (5.14), the first factor of (5.22) is unconditionally non-negative, independently of the values of $F^2$ and $G^2$. The second factor is also found to be non-negative when

$$\alpha^2 \geq \Phi_0\left(\frac{\Delta t}{2}\right)^2. \tag{5.23}$$

In summary, provided conditions (5.23) hold, $|E|^2 = 1$ from (5.20) - (5.22), and the discretisation is neutrally stable.

# 6 An example application

To demonstrate the behaviour of the proposed scheme under a nonlinear, nearly balanced flow regime, the shallow-water equations (2.1)-(2.3) are considered on an $f$-plane placed at $45^o$ degree latitude and within a doubly periodic domain of length $L_x = L_y = 3840\,\mathrm{km}$. Initial conditions for $(u, v, \Phi)$ are chosen to satisfy the reverse balance equation

$$\nabla^2\Phi = f(v_x - u_y) - 2J(u, v), \tag{6.1}$$

where $J(u, v) \equiv v_x u_y - u_x v_y$ denotes the Jacobian operator. The reference height of the fluid is set equal to 9665 m, i.e., $\Phi_0 \approx 9.4814 \times 10^4\,\mathrm{m^2\,s^{-2}}$. The initial conditions are furthermore chosen such that two interacting vortices are generated. See Fig. 1 for the initial fluid height $h$, and the uppermost panels of Fig. 2 for the initial potential vorticity (PV) field $q \equiv (v_x - u_y + f)/h$. The maximum initial wind speed is approximately $11\,\mathrm{m\,s^{-1}}$.

The time-staggered semi-Lagrangian discretisation, described and analysed in Sections 4 and 5.2 respectively, has been implemented on an Arakawa C grid - see Appendix A for details. The gridlength is $\Delta x = \Delta y = 60\,\mathrm{km}$, the timestep is $\Delta t = 20\,\mathrm{min}$, and the regularisation parameter $\alpha$ is set to its optimal value $\alpha^2 = \Phi_0(\Delta t/2)^2$. Trajectory computations are implemented as fixed point iterations with two iterations per trajectory computation. To assess the time-staggered semi-Lagrangian discretisation, an additional simulation is performed using the well-established two-time-level semi-implicit semi-Lagrangian approach

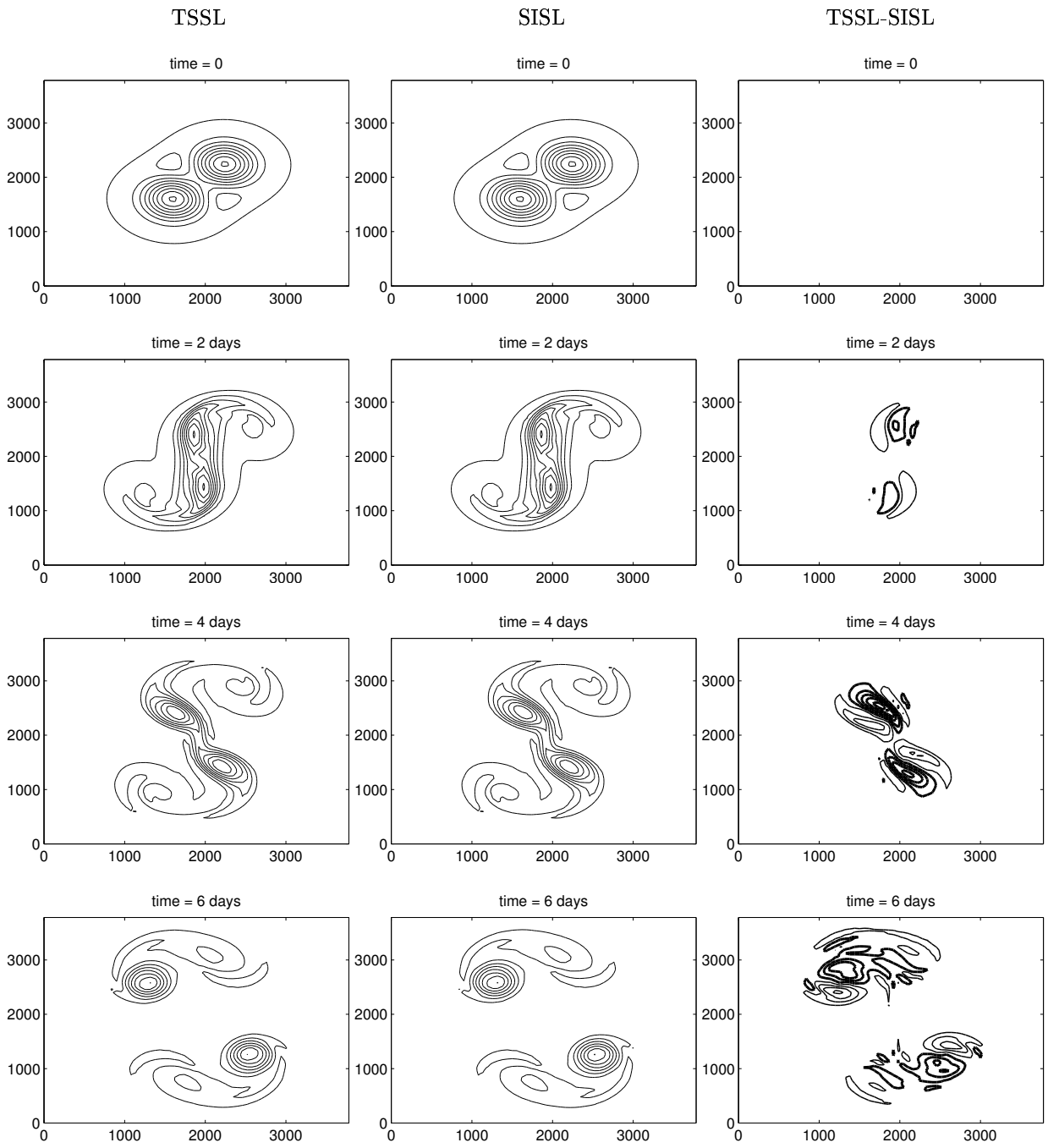


Figure 2: Computed time evolution, from initial time to $t = 6$ days, of PV over the domain $(x, y) \in [0, 3840\,\mathrm{km}] \times [0, 3840\,\mathrm{km}]$ using the time-staggered semi-Lagrangian (leftmost panels) and semi-implicit semi-Lagrangian (centre panels) schemes, both with timestep $\Delta t = 20\,\mathrm{min}$: contours plotted between $6.4 \times 10^{-8}\,\mathrm{m^{-1}s^{-1}}$ and $2.2 \times 10^{-7}\,\mathrm{m^{-1}s^{-1}}$ with contour interval $1.56 \times 10^{-8}\,\mathrm{m^{-1}s^{-1}}$. Differences (time-staggered semi-Lagrangian minus semi-implicit semi-Lagrangian) at corresponding times are plotted in rightmost panels with a 10 times smaller contour interval, where thin (thick) lines are positive (negative) contours.

[e.g. Temperton & Staniforth (1987), McDonald & Bates (1987)], implemented here on an Arakawa C grid. This integration is also performed using a timestep of $\Delta t = 20\,\mathrm{min}$, which is an order-of-magnitude larger than the stability limit ($\Delta t \sim 1.5\,\mathrm{min}$) of a traditional explicit Eulerian leapfrog time scheme. As can be seen from Fig. 2, both simulations yield very similar results.

# 7 Conclusions

A recently proposed, time-staggered and regularised temporal discretisation of the non-advective SWEs has been coupled with a semi-Lagrangian scheme for advection. Linear analysis shows that the scheme is unconditionally stable provided the regularisation parameter is chosen in the same way as for the non-advective case.

The scheme has been spatially discretised on an Arakawa C-grid and is second-order accurate in both time and space. Its application to a fully nonlinear example of two interacting vortices demonstrates the practical potential of the scheme for the stable discretisation of the SWE's.

It is known that centred semi-implicit semi-Lagrangian discretisations of the SWE's can suffer from spurious resonance at large timestep in the presence of orography (Rivest et al. 1994). It is therefore important to include orography in the present scheme, and to analyse the forced response. This is done in a companion Note (Staniforth & Wood 2006) to the present one. Therein it is shown that the obvious extension of the present scheme can also exhibit spurious orographic resonance. However, it is also shown that this can be addressed, without adversely affecting stability, by using a procedure akin to the off-centring one proposed in Rivest et al. (1994).

# References


Frank, J., Reich, S., Staniforth, A., White, A. & Wood, N. 2005 , Analysis of a regularized, time-staggered discretization method and its link to the semi-implicit method, *Atmos. Sci. Letters* **6**, 97–104.

McDonald, A. & Bates, J. R. 1987 , Improving the estimate of the departure point in a two-time level semi-Lagrangian and semi-implicit scheme, *Mon. Wea. Rev.* **115**, 737–739.

Rivest, C., Staniforth, A. & Robert, A. 1994 , Spurious resonant response of semi-Lagrangian discretizations to orographic forcing: diagnosis and solution, *Mon. Wea. Rev.* **122**, 366–376.

Staniforth, A. 1997 , André Robert (1929 - 1993): His Pioneering Contributions to Numerical Modelling, *in* C. A. Lin, R. Laprise & H. Ritchie, eds, 'Numerical Methods in Atmospheric and Oceanic Modelling, The André J. Robert memorial volume', CMOS/ NRC Press, Ottawa, pp. 25–54.

Staniforth, A. & Côté, J. 1991 , Semi-Lagrangian integration schemes for atmospheric models - a review, *Mon. Wea. Rev.* **119**, 2206–2223.

Staniforth, A. & Wood, N. 2006 , Analysis of the response to orographic forcing of a TSSL discretization of the rotating SWEs, *Q. J. R. Meteorol. Soc.* (to appear).

Temperton, C. & Staniforth, A. 1987 , An efficient two-time-level semi-Lagrangian semi-implicit integration scheme, *Q. J. R. Meteorol. Soc.* **113**, 1025–1039.

Wood, N., Staniforth, A. & Reich, S. 2006 , An improved regularization for time-staggered discretization and its link to the semi-implicit method, *Atmos. Sci. Letters* **7**, 21–25.


# A Implementation details for a C grid

Consider a doubly periodic domain $(x, y) \in [0, L] \times [0, L]$. The spatial discretisation of the shallow-water equations is performed using a standard Arakawa C grid with gridlengths $\Delta x = \Delta y = L/N$, where $N$ is the number of independent integer points in each direction. For all $i, j = 0, \ldots, N-1$, integer gridpoints are located at $(x_i, y_j) = (i\Delta x, j\Delta y)$, cell-centred grid points at $\left(x_{i+1/2}, y_{j+1/2}\right) = \left((i + 1/2)\,\Delta x, (j + 1/2)\,\Delta y\right)$, and a

pair of side-centred grid points at $(x_{i+1/2}, y_i) = ((i+1/2)\,\Delta x, j\Delta y))$ and $(x_i, y_{j+1/2}) = (i\Delta x, (j+1/2)\,\Delta y)$. Following standard practice, the geopotential $\Phi$ is stored at cell-centred grid points $(x_{i+1/2}, y_{j+1/2})$, with numerical values denoted by $\Phi_{i+1/2,j+1/2}$. Similarly, the $u$ and $v$ velocity components are stored at the side-centred grid points $(x_i, y_{j+1/2})$ and $(x_{i+1/2}, y_j)$ respectively, with corresponding numerical values denoted by $u_{i,j+1/2}$ and $v_{i+1/2,j}$.

Define differencing operators

$$(\delta_x \mathcal{F})_{m,n} = \frac{\mathcal{F}_{m+\frac{1}{2},n} - \mathcal{F}_{m-\frac{1}{2},n}}{\Delta x}, \quad (\delta_y \mathcal{F})_{m,n} = \frac{\mathcal{F}_{m,n+\frac{1}{2}} - \mathcal{F}_{m,n-\frac{1}{2}}}{\Delta y}, \tag{A.1}$$

and averaging operators

$$\overline{\mathcal{F}}^x_{m,n} = \frac{1}{2}\left(\mathcal{F}_{m+\frac{1}{2},n} + \mathcal{F}_{m-\frac{1}{2},n}\right), \quad \overline{\mathcal{F}}^y_{m,n} = \frac{1}{2}\left(\mathcal{F}_{m,n+\frac{1}{2}} + \mathcal{F}_{m,n-\frac{1}{2}}\right), \tag{A.2}$$

where $\mathcal{F}$ denotes any variable stored at appropriate gridpoints, with $m$ and $n$ being either integers or half integers as appropriate. One can combine these operators to obtain composite differencing and averaging operators such as

$$\left(\delta_x^2 \Phi\right)_{i+\frac{1}{2},j+\frac{1}{2}} = \frac{\Phi_{i+\frac{3}{2},j+\frac{1}{2}} - 2\Phi_{i+\frac{1}{2},j+\frac{1}{2}} + \Phi_{i-\frac{1}{2},j+\frac{1}{2}}}{\Delta x^2} \tag{A.3}$$

and

$$\overline{v}^{xy}_{i,j+\frac{1}{2}} = \frac{1}{4}\left(v_{i+\frac{1}{2},j} + v_{i-\frac{1}{2},j} + v_{i+\frac{1}{2},j+1} + v_{i-\frac{1}{2},j+1}\right) \tag{A.4}$$

with analogous expressions for $\left(\delta_y^2 \Phi\right)_{i+1/2,j+1/2}$ and $\overline{u}^{xy}_{i+1/2,j}$, respectively.

Applying this spatial discretisation to (3.1) - (3.5) gives

$$\frac{D}{Dt} u_{i,j+\frac{1}{2}} = +f\bar{v}^{xy}_{i,j+\frac{1}{2}} - \left(\delta_x \tilde{\Phi}\right)_{i,j+\frac{1}{2}}, \tag{A.5}$$

$$\frac{D}{Dt} v_{i+\frac{1}{2},j} = -f\bar{u}^{xy}_{i+\frac{1}{2},j} - \left(\delta_y \tilde{\Phi}\right)_{i+\frac{1}{2},j}, \tag{A.6}$$

$$\frac{D}{Dt}\left(\ln \Phi\right)_{i+\frac{1}{2},j+\frac{1}{2}} = -\left(\delta_x u + \delta_y v\right)_{i+\frac{1}{2},j+\frac{1}{2}}, \tag{A.7}$$

where the regularised geopotential is defined by

$$\left\{\left[1 - \alpha^2\left(\delta_x^2 + \delta_y^2\right)\right]\left(\tilde{\Phi} - \Phi\right)\right\}_{i+\frac{1}{2},j+\frac{1}{2}} = -\alpha^2\left(\delta_x R^u + \delta_y R^v\right)_{i+\frac{1}{2},j+\frac{1}{2}}, \tag{A.8}$$

and

$$R^u_{i,j+\frac{1}{2}} \equiv f\overline{v}^{xy}_{i,j+\frac{1}{2}} - \left(\delta_x \Phi\right)_{i,j+\frac{1}{2}}, \qquad R^v_{i+\frac{1}{2},j} \equiv -f\overline{u}^{xy}_{i+\frac{1}{2},j} - \left(\delta_y \Phi\right)_{i+\frac{1}{2},j}. \tag{A.9}$$

These equations can be combined to yield a single equation

$$\left\{\left[1 - \alpha^2\left(\delta_x^2 + \delta_y^2\right)\right]\tilde{\Phi}\right\}_{i+\frac{1}{2},j+\frac{1}{2}} = \left[\Phi - \alpha^2 f\left(\delta_x \overline{v}^{xy} - \delta_y \overline{u}^{xy}\right)\right]_{i+\frac{1}{2},j+\frac{1}{2}}. \tag{A.10}$$

To apply the spatial C-grid discretisation with the time-staggered semi-Lagrangian temporal one of section 4 requires specification of the discrete trajectory equations used to determine departure points. For simplicity, three sets of trajectories are computed in the present implementation, viz. those for particles that arrive at cell-centred gridpoints $(x_{i+1/2}, y_{i+1/2})$, and at side-centred gridpoints $(x_{i,j+1/2}, y_{i,j+1/2})$ and $(x_{i+1/2,j}, y_{i+1/2,j})$. The relevant discretisations at time level $t^n$ for the $(u, v)$ trajectories of the momentum equation (4.1) are

$$\frac{\left(x_{i,j+\frac{1}{2}}, y_{i,j+\frac{1}{2}}\right) - \left(x_{i,j+\frac{1}{2}}, y_{i,j+\frac{1}{2}}\right)^{n-1}_D}{\Delta t} = \frac{1}{2}\left[\left(u_{i,j+\frac{1}{2}}, \overline{v}^{xy}_{i,j+\frac{1}{2}}\right)^n_A + \left(u_{i,j+\frac{1}{2}}, \overline{v}^{xy}_{i,j+\frac{1}{2}}\right)^{n-1}_D\right], \tag{A.11}$$

$$\frac{\left(x_{i+\frac{1}{2},j}, y_{i+\frac{1}{2},j}\right) - \left(x_{i+\frac{1}{2},j}, y_{i+\frac{1}{2},j}\right)^{n-1}_D}{\Delta t} = \frac{1}{2}\left[\left(\overline{u}^{xy}_{i+\frac{1}{2},j}, v_{i+\frac{1}{2},j}\right)^n_A + \left(\overline{u}^{xy}_{i+\frac{1}{2},j}, v_{i+\frac{1}{2},j}\right)^{n-1}_D\right]. \tag{A.12}$$

The corresponding discretisation for the trajectories of the continuity equation (4.4) is

$$\frac{(x_{i+\frac{1}{2},j+\frac{1}{2}}, y_{i+\frac{1}{2},j+\frac{1}{2}}) - (x_{i+\frac{1}{2},j+\frac{1}{2}}, y_{i+\frac{1}{2},j+\frac{1}{2}})_D^{n-\frac{1}{2}}}{\Delta t} = \frac{1}{2}\left[\left(\overline{u}^x_{i+\frac{1}{2},j+\frac{1}{2}}, \overline{v}^y_{i+\frac{1}{2},j+\frac{1}{2}}\right)_A^n + \left(\overline{u}^x_{i+\frac{1}{2},j+\frac{1}{2}}, \overline{v}^y_{i+\frac{1}{2},j+\frac{1}{2}}\right)_D^n\right]. \tag{A.13}$$